A SCALE INVARIANCE MODEL FOR SPATIAL DOWNSCALING OF TOPOGRAPHIC INDEX IN TOPMODEL

Nawa Raj PRADHAN[1], Yasuto TACHIKAWA[2] and Kaoru TAKARA[3]

[1]Student member of JSCE, Graduate Student, Dept. of Civil Eng., Kyoto University, (Yoshida Honmachi, Sakyo-ku, Kyoto, 606-8501, Japan)
[2]Member of JSCE, Dr. Eng., Associate Professor, DPRI, Kyoto University, (Gokasho, Uji, 611-0011, Japan)
[3]Fellow of JSCE, Dr. Eng., Professor, DPRI, Kyoto University, (Gokasho, Uji, 611-0011, Japan)

Failure to translate scale dependencies of dominating geomorphometric parameters into effective hydrological models has posed a serious problem for ungauged basins where only coarse resolution elevation data is available. To overcome this problem, scale laws that govern the relation in digital elevation data resolution on geomorphometric parameters of topographic index of TOPMODEL have been analyzed. A scale invariance model for down scaling of topographic index distribution has been developed by introducing a resolution factor and a fractal method for the scaled steepest slope in topographic index. The method successfully derived topographic index distribution of fine resolution DEM by using only coarse resolution DEM. The scale invariance model has been applied to Kamishiiba catchment (210 km^2) and it is shown that the down scaled topographic index distribution is similar to a target topographic index distribution.

Key Words: *Scale invariance, down scale, fractal method, topographic index distribution*

1. INTRODUCTION

Despite the enormous capacity of today's (and tomorrow's) information technologies, the complexity of the Earth's surface is such that the most voluminous descriptions are still only coarse generalizations of what is actually present [1]. This implies that the need for continued and sustained research on scale issues is therefore self-evident. In the field of hydrology, the desire to develop more physically realistic distributed models has been motivated for forecasting changes in hydrological behavior due to a variety of land use and climate changes and for hydrologic predictions in ungauged basins. An important part of this goal is to replace the dependence of models on calibrated 'effective parameters' with physically realistic process descriptions that use parameters inferred from the direct observation of land surface conditions. As the spatial extent is expanded beyond point experiments to larger watershed regions, the direct extension of the point models requires an estimation of the distribution of model parameters and process computations over the heterogeneous land surface. If a distribution of a set of spatial variables required for a given hydrological model (e.g. surface slope, soil hydraulic conductivity) can be described by a joint density function, then digital elevation models (DEMs) and geographical information systems (GISs) may be evaluated as a tool for estimating this function. Now the question to be asked is whether current GISs and current available spatial data sets are sufficient to adequately estimate these density functions. Several researches [2),3),4)] have discussed the effects of digital elevation model map scale and data resolution on the distribution of the topographic index, concluding that there is interdependence between DEM scale and topographic index distribution. Although these researches have demonstrated significant results concerning scale dependencies, they fail to translate these relations into effective hydrological models which have posed a serious problem for the ungauged basins of developing countries where only coarse resolution DEM data, e.g. 30 arc second resolution DEM data set in GTOPO30, USGS web site, is available [5]. Band et al. [6] point out that higher frequency topographic information is lost as the larger

sampling dimensions of the grids act as filter. This is one of the nature and extent of the scale problem and without its solution it is even more serious to prediction in ungauged basins. If this argument is accepted the hydrological modelers should seek methods to acquire a more realistic subgrid scale parameterization.

In this study we focus on the influence of DEM resolution on dominating geomorphometric parameters - such as slope angle, upslope contributing area, which are considered as the main controls in a number of hydrological processes - and develop a scale invariance model by incorporating scaling laws that can bridge the gap between scaling issues. By using the model, the topographic index distribution of fine resolution DEM is successfully derived by using only coarse resolution DEM.

2. METHODOLOGY

Topographic index of TOPMODEL is defined as

$$I = \ln\left\{\frac{a}{(\tan\beta)}\right\} \quad (1)$$

where a is the local up-slope catchment area per unit contour length and β is the slope angle of the ground surface. TOPMODEL allows for spatial heterogeneity by making calculations on the basis of the topographic index distribution. Topographic index is scale dependent which leads identified parameter values to be dependent on DEM resolution. This makes difficult to use model parameter values identified with different resolution model. To overcome the problem, scale invariant model of topographic index is proposed. To scale upslope contributing area per unit contour length a and slope angle of the ground surface β, resolution factor and scaled slope with fractal method is introduced.

(1) Theory of TOPMODEL

The topographic index defined by equation (1) describes the tendency of water to accumulate and to be moved down slope by gravitational forces. For steep slopes at the edge of a catchment, a is small and β is large which yields a small value for the topographic index. High index values are found in areas with a large up-slope area and a small slope, e.g. valley bottoms. The TOPMODEL theory can be formulated by the concept of local saturation deficits (water needed for saturation up to surface).

Following Beven and Kirkby [7] subsurface flow rate $q_b(i,t)$ can be related to local soil storage deficit $SD(i,t)$ by

$$q_b(i,t) = K_i \tan\beta_i e^{-SD(i,t)/m} \quad (2)$$

where, i is any point in a catchment, $\tan\beta_i$ is local slope angle, K_i is lateral transmissivity or soil transmissivity and m is a decay factor of lateral transmissivity with respect to saturation deficit. When a steady condition is assumed

$$a_i R = K_i \tan\beta_i e^{-SD(i,t)/m} \quad (3)$$

where, R is steady input, a_i is the area draining through i per unit contour length. Equation (3) can be rearranged to equation (4).

$$SD(i,t) = -m\left[\ln\left\{\frac{a_i}{(K_i \tan\beta_i)}\right\} + \ln R\right] \quad (4)$$

Average saturation deficit over the entire area $\overline{SD(t)}$ is

$$\overline{SD(t)} = \frac{1}{A}\int_A SD(i,t) = -m(\gamma + \ln R) \quad (5)$$

where, $\gamma = \frac{1}{A}\int_A \ln\left\{\frac{a_i}{(K_i \tan\beta_i)}\right\}$, a constant for the basin. Equation (4) and (5) yield a relation between $\overline{SD(t)}$ and $SD(i,t)$ at each single location i.

$$SD(i,t) = \overline{SD(t)} + m\left[\gamma - \ln\left\{\frac{a_i}{(K_i \tan\beta_i)}\right\}\right] \quad (6)$$

Underlying the development of equation (6) is an assumption that all points with the same $\ln(a_i/K_i \tan\beta_i)$ value are hydrologically similar [8]. Subsurface contributions to streamflow, Q(t) – flow per unit area [8] – can be derived from equation (6) as

$$Q(t) = e^{-\gamma} e^{-\overline{SD}(t)/m} \quad (7)$$

Considering lateral transitivity to be constant in a block [5),9)] or subcatchment, then the key role for hydrological similar condition is played by the distribution function of topographic index. The bitter fact is that higher frequency topographic information contained in topographic index is lost as the larger sampling dimensions of the grids act as filter. This makes the hydrological similarity condition accounting combined soil-topographic index, $\ln(a_i/K_i \tan\beta_i)$, to vary with the variation in DEM resolution used. To overcome this problem, this research has developed a scale invariance model structure for topographic index.

(2) Influence of DEM resolution on topographic index

Figure 1 shows the density function of the topographic index at four different DEM resolutions in Kamishiiba catchment (210 km^2) without taking into account the scale effect. Distinct swift of topographic index density function towards the higher value is seen as the resolution of DEM gets coarser. This is a clear indication of the lost of higher frequency topographic information as the larger sampling dimensions of the grids act as filter.

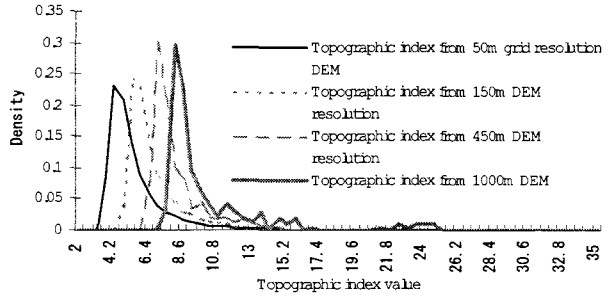

Fig. 1 Effect of DEM resolution on density distribution of topographic index.

Table 1 DEM resolution effect on topographic constant, λ, value in Kamishiiba catchment

DEM Resolution	50 m	150 m	450 m	600 m	1000 m
Topographic constant λ	6.076	7.423	9.222	9.622	10.353

Table 1 shows the distinct effect of DEM resolution on topographic constant, $\lambda = \frac{1}{A}\int_A \ln(a_i/\tan\beta_i)$, of Beven and Kirkby [7].

Only available DEM data for most of the parts of the world that covers ungauged basins of developing and underdeveloped countries is that of 1km x 1km grid resolution. Analyzing Fig. 1 and Table 1, we can readily imagine the blunder in predicting ungauged basins using coarse resolution DEM.

(3) Scale Invariant Model for topographic index of TOPMODEL

A scale invariant model for topographic index of TOPMODEL has been developed by combining two parts of solutions as follows:

i) Resolution factor in topographic index

The density of the small contributing area is higher in a catchment. It is observed that this small contributing area is entirely lost when the resolution of DEM gets coarser. Figure 1 clarifies that higher frequency topographic information contained in topographic index is lost. In Fig. 1 the peak of density distribution of topographic index for 50m grid resolution DEM is at the topographic index value 4.2 and the peak of density distribution of topographic index for 1000m grid resolution DEM is at the topographic index value 8.6. In fact the smallest contributing area derived from a DEM resolution is a single grid of the DEM at that resolution. Thus area smaller than this grid resolution is completely lost as the larger sampling dimensions of the grids act as filter. But as we use finer resolution DEM, the smaller contributing area - that is the area of finer grid resolution is achieved. From this point of view we introduced number of sub grids N_s (see Fig. 2) concept in topographic index as shown in equation (8).

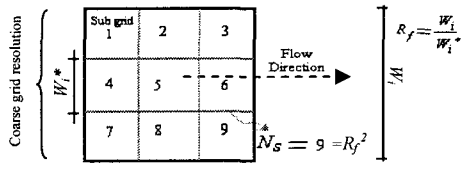

Fig. 2 Sub grids within coarse grid resolution for introducing resolution factor in topographic index.

$$TI = \ln\left\{\frac{C_i}{(W^*_i N_s \tan\beta_i)}\right\} \quad (8)$$

where TI is topographic index. C_i is the upslope contributing area of the coarse resolution DEM and W^*_i is the unit contour length of target resolution DEM. N_s is the total number of subgrids within a coarse resolution grid. i is a location in a catchment.

Figure 2 shows 9 subgrids within a coarse resolution grid. The area of the coarse resolution grid shown in Fig. 2 itself is the smallest contributing area for that DEM resolution. When this area of coarse resolution DEM is divided by the number of sub grids (i.e. 9 in Fig. 2), area of a sub grid as smallest contributing area for the target DEM resolution is obtained. Moreover, in equation (8), the unit contour length of coarse resolution DEM, W_i, is replaced by the unit contour length of targeted DEM resolution W^*_i (see Fig. 2) to derive the lost portion of the finer values of contributing area per unit contour length.

The density distribution of the higher values of contributing area per unit contour length is found lower in case of finer grid resolution DEM than that of coarser grid resolution DEM. This is the reason for the topographic index derived from coarser resolution DEM to swift towards the higher value throughout the density distribution, not only at the peak of the density distribution, than the topographic index derived from finer resolution DEM (see Fig. 1). Structure of equation (8) having logarithmic function, proportionately pulled back this higher topographic index density towards that of finer resolution DEM.

If we consider resolution factor R_f as :

$$R_f = \frac{Coarse\ \ DEM\ \ \text{Re}\ solution}{T\ \text{arg}\ et\ \ DEM\ \ \text{Re}\ solution} = \frac{W_i}{W^*_i} \quad (9)$$

then it is clear from Fig. 2 that

$$N_s = R_f^2 \quad (10)$$

Equation (9) and (10) yield

$$W_i R_f = W^*_i N_s \quad (11)$$

From, equation (8) and equation (11) resolution factor is introduced in topographic index as:

$$TI = \ln\left\{\frac{C_i}{(W_i R_f \tan\beta_i)}\right\} \quad (12)$$

ii) Fractal method for scaled steepest slope

The underestimation of slopes when using the coarse resolution DEMs can seriously affect the accuracy of hydrologic and geomorphological

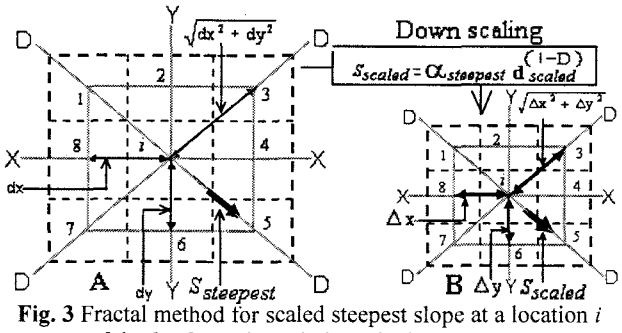

Fig. 3 Fractal method for scaled steepest slope at a location *i* of the 3 x 3 moving window pixels.

models [10]. To scale the local slope, we followed the fractal theory in topography and slope proposed by Klinkenberg and Goodchild [11] and Zhang et al. [10] and developed a modified fractal method for steepest descent slope.

a) Fractal method for average slope estimation proposed by Zhang et al. [10]

The variogram technique (statistical variation of the elevations between samples varies with the distance between them) can be used to calculate the fractal dimension in a region when the log of the distance between samples is regressed against the log of the mean squared difference in the elevations for that distance [11].

The variogram equation used by Klinkenberg and Goodchild [11] to calculate the fractal dimension of topography is:

$$(Z_p - Z_q)^2 = k d_{pq}^{(4-2D)} \qquad (13)$$

where Z_p and Z_q are the elevations at points p and q, d_{pq} is the distance between p and q, k is a constant and D is fractal dimension. Topographic fractal properties of equation (13) can be used to scale slope as follows:

$$\frac{(Z_p - Z_q)}{d_{pq}} = \alpha d_{pq}^{(1-D)} \qquad (14)$$

where $\alpha = \pm k^{0.5}$ is a constant. Because the left part of the above equation represents the surface slope, it can be assumed that the slope value S is associated with its corresponding scale (grid size) d by the equation:

$$S = \alpha d^{(1-D)} \qquad (15)$$

This implies that if topography is unifractal in a specified range of measurement scale, slope will then be a function of the measurement scale [10]. However, it is impossible to predict the spatial patterns of slopes due to the single value of the fractal dimension and the coefficient in the fractal slope equation for the whole DEM. To overcome this problem Zhang et al. [10] proposed that the coefficient α and fractal dimension D of equation (15) are mainly controlled by standard deviation (σ) of the elevation of the sub regions in a DEM and brought out the regressed relations between α and D separately with the standard deviation (σ) of the elevation. In deriving the regressed relation, Zhang et al. [10] considered the smallest sub area (window) to be composed of 3 x 3 pixels. Hence elevations of nine neighboring grids in the DEM are taken to obtain the standard deviation of the elevation for a sub area.

It is found that the slope derived from the method by Zhang et al. [10] tend to match only with the average slope within the 3 x 3 moving window pixels of the coarse resolution DEM but completely failed to take into consideration of the steepest descent slope defined as the direction of the maximum drop from centre pixel to its eight nearest neighbors. Steepest descent slope also known as D8 method has a significant role in hydrological modeling that incorporates DEM. Thus we propose a modified fractal method for steepest descent slope.

b) Fractal method for steepest descent slope

In this research, a modified model for Fractal method to account for the steepest slope change due to change in DEM resolution has been developed which is described in the following points:

b1) Unlike distance d of equation (15) be represented by constant grid size, in every step (location) in a 3 x 3 moving window pixels, this distance 'd' of equation (15) is provided as the steepest slope distance ($d_{steepest}$). Figure 3-A shows the steepest slope distance ($d_{steepest}$) to be dx, dy and $\sqrt{dx^2 + dy^2}$ according to the direction of steepest descent of the slope in X-axis, Y-axis and diagonal axis DD respectively.

b2) It is found that there is not much variation in standard deviation from high resolution DEM to low resolution DEM in the same sub-area. Fractal dimension D is related to standard deviation in 3 x 3 moving window pixels as per Zhang et al [11].

$$D = 1.13589 + 0.08452 \ln \sigma \qquad (16)$$

b3) The fluctuations of the coefficient α values were found very high from one local place to another in comparison to D value in equation (15). Unlike the method by Zhang et al. [10] (α values are derived from standard deviation σ of the elevation in 3 x 3 moving window pixels), coefficient α values are derived directly from the steepest slope (steepest slope of the available coarse resolution DEM), keeping the fact that steepest slope itself represents the extreme fluctuation. The modified equation is:

$$S_{steepest} = \alpha_{steepest} d_{steepest}^{(1-D)} \qquad (17)$$

As for example in Fig 3-A, where the steepest slope is shown in diagonal direction, $\alpha_{steepest}$ at that location i is given by

$$\alpha_{steepest} = \frac{S_{steepest}}{\left(\sqrt{dx^2 + dy^2}\right)^{(1-D)}}$$

where dx and dy are the steepest slope distances of the coarse resolution DEM in X-axis and Y-axis.

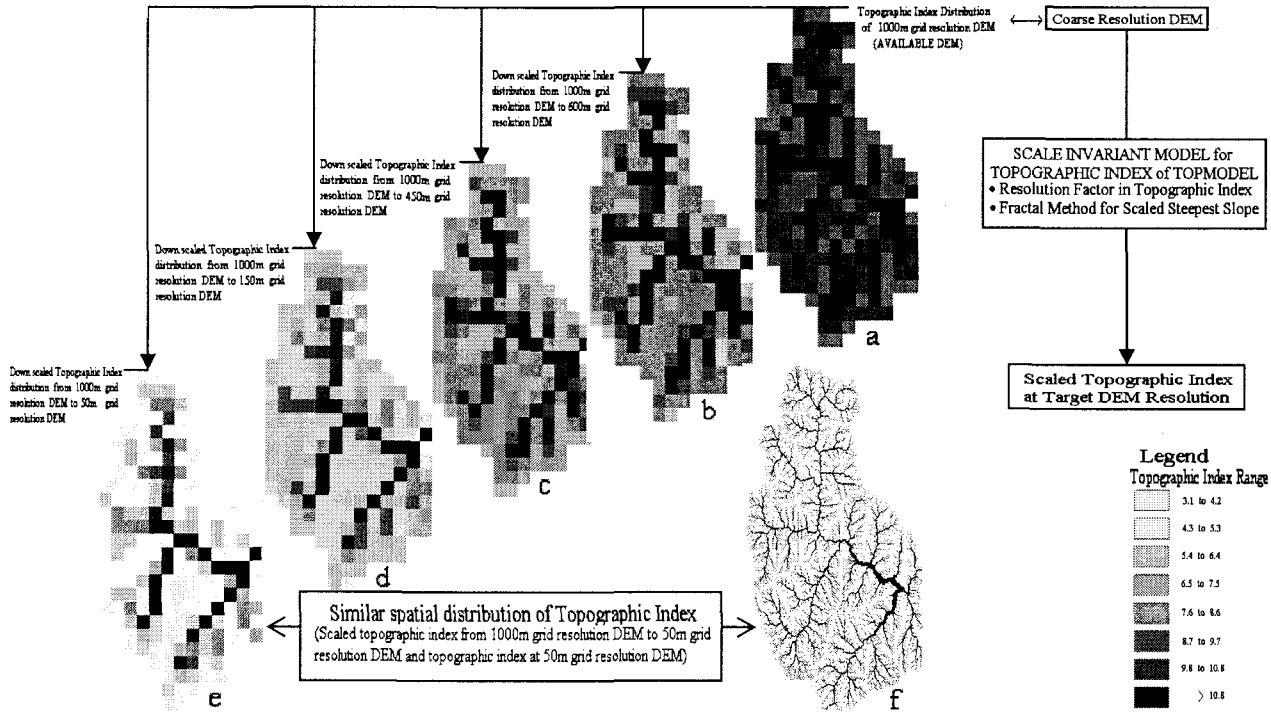

Fig. 4 Spatial distribution of scaled topographic index applied to Kamishiiba catchment (210 km^2). (a) topographic index distribution using 1000m DEM resolution, (b) scaled topographic index distribution obtained from 1000m DEM resolution to 600m DEM resolution, (c) scaled topographic index distribution from 1000m DEM resolution to 450m DEM resolution, (d) scaled topographic index distribution from 1000m DEM resolution to 150m DEM resolution, (e) scaled topographic index distribution from 1000m DEM resolution to 50m DEM resolution, (f) topographic index distribution using 50m DEM

b4) While down scaling, the distance variation in the target resolution DEM is made as per the direction of the steepest slope in the coarse resolution DEM. Hence in Fig. 3-B the down scaled steepest slope (S_{scaled}) is shown in the same direction to that of the coarse resolution DEM steepest slope (Fig. 3-A). Considering Fig. 3-B, the down scaled steepest slope (S_{scaled}) is given as

$$S_{scaled} = \alpha_{steepest} d_{scaled}^{(1-D)} \tag{18}$$

where $d_{scaled} = \sqrt{\Delta x^2 + \Delta y^2}$ in Fig. 3-B and Δx, Δy are the steepest slope distances of the target resolution DEM in X-axis and Y-axis respectively.

iii) Scaled topographic index distribution

By combining equation (12) and equation (18), final scale invariant model for the scaled topographic index which includes resolution factor to account for the effect of scale in up slope contributing area per unit contour length and a fractal method for scaled steepest slope as an approach to account for the effect of scale on slope is given by equation (19).

$$(TI)_{scaled} = \ln\left[\frac{C_i}{\{W_i R_f (\tan\beta_i)_F\}}\right] \tag{19}$$

where, $(TI)_{scaled}$ is the scaled topographic index and $(\tan\beta_i)_F = S_{scaled}$ of equation (18) which is the scaled steepest slope by fractal method.

Table 2 Topographic constant, λ, value for scaled DEM from 1000 m grid resolution to finer grid resolutions in Kamishiiba catchment

Topographic constant, λ, value for scaled DEM from 1000 m grid resolution to			
50 m target grid resolution	150 m target grid resolution	450 m target grid resolution	600 m target grid resolution
6.474	7.573	9.11	9.604

3. RESULTS AND DISCUSSION

The scale invariant model of topographic index of TOPMODEL is applied to Kamishiiba catchment (210 km^2). Table 2 shows the scaled topographic constant λ from 1000m grid resolution DEM to various DEM resolutions by applying the scale invariant model. The down scaled values of λ from 1000m grid resolution to finer DEM resolutions in Table 2 are almost equal to the values of λ in Table 1 derived from that fine grid resolution DEMs.

Figure 4, (a) is the topographic index distribution using 1000m DEM. Figures 4 (b), (c), (d) and (e) are the scaled topographic index distribution obtained by using the scale invariant model from the same 1000m grid resolution DEM to 600m, 450m, 150m and 50m grid resolution DEM respectively. Figure 4 (f) is the topographic index distribution using 50m DEM. Distinct difference can be seen between spatial distribution of topographic index (a)

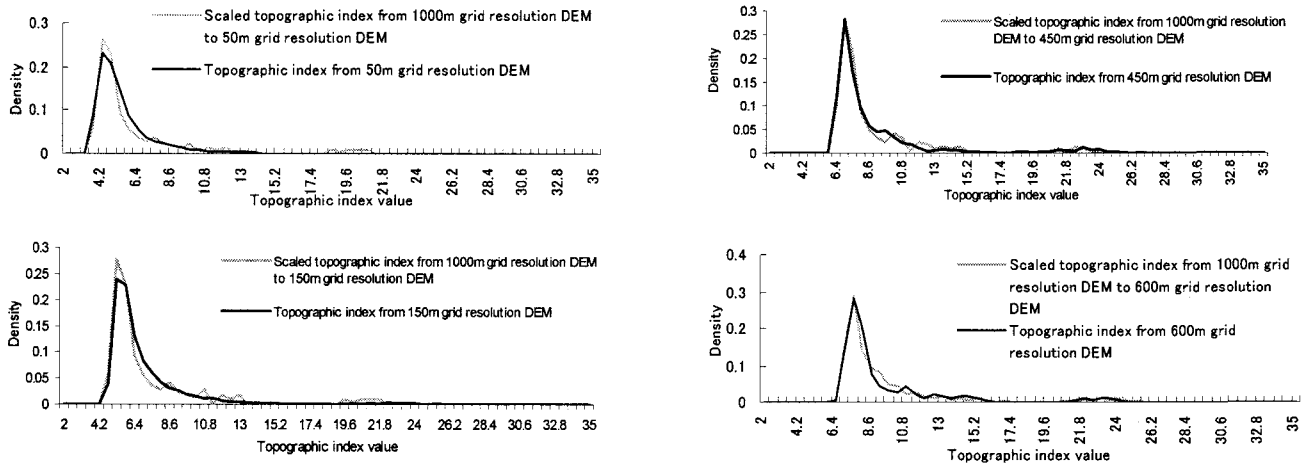

Fig. 5 Comparison of density function of scaled topographic index from 1000m grid resolution DEM to finer grid resolution DEM and the density function of the topographic index at that fine scale in Kamishiiba catchment (210 km^2).

and (f) that are from 1000m grid resolution DEM and 50m grid resolution DEM. The spatial distribution of topographic index displayed by (e) has matched the existing reality displayed by (f) in Fig. 4.

Figure 5 shows the perfect fit of density function of scaled topographic index distribution from 1000m grid resolution DEM to various grid resolution DEMs by using scale invariant model. It is found that in the finer resolution range of DEM, between 50m grid resolution DEM and 150m grid resolution DEM where the slope obtained is more precise and does not vary significantly, resolution factor (R_f) alone played the dominant role in the scale invariant model. Above 150m DEM scale, effect of resolution on slope is found distinct.

4. CONCLUSION

According to the present research objective a scale invariant model for topographic index has been developed and its applicability has been highlighted as a tool to help prediction in ungauged basins in a realistic manner. This research has developed concept of resolution factor to account for the effect of scale in up slope contributing area per unit contour length in topographic index and a fractal method for scaled steepest slope as an approach to account for the effect of scale on slopes, which are combined to develop scale invariant model of topographic index distribution. It is hoped that the findings of this research seeks its applicability as a tool to a wider range of boundary as per the scale problems in hydrology and solution approach is concerned.

REFERENCES

1) Goodchild, M. F., Models of Scale and Scales of Modelling: *Modelling Scale in Geographical Information Science*, edited by N. J. Tate and P. M. Atkinson, John Wiley & Sons Ltd, Chichester, 3-10, 2001.

2) Quinn, P., Beven, K., Chevallier, P. and Planchon, O. The prediction of hillslope flow paths for distributed hydrological modeling using digital terrain models, *Hydrol. Process.*, 5, 59-79,1991.

3) Wolock, D. M. & Price, C. V., Effects of digital elevation model map scale and data resolution on a topography based watershed model, *Wat. Resour. Res.* 30(11), 3041-3052, 1994.

4) Zhang, W. and Montgomery, D. R., Digital elevation model grid size, landscape representation, and hydrologic simulations. *Wat. Resour. Res.* 30(4), 1019-1028.

5) Pradhan, N. R. and Jha, R., Performance assessment of BTOPMC model in a Nepalese drainage basin, Weather radar information and distributed hydrological modeling , IAHS publication no. 282, 288-293, 2003.

6) Band, L. E. and Moore, I. D., Scale: Landscape attributes and geographical information systems: *Scale Issues in Hydrological Modelling*, edited by J. D. Kalma and M. Sivapalan, Wiley & Sons Ltd, Chichester, 159-179, 1995.

7) Beven, K. J. and Kirkby, M. J., A physically based, variable contributing area model of basin hydrology, *Hydrol. Sci Bull.* 24, 43-69, 1979.

8) Beven, K., Runoff production and flood frequency in catchments of order n: An alternative approach: *Scale Problems in Hydrology*, edited by V. K. Gupta, I. Rodríguez-Iturbe and E. F. Wood, D. Reidel Publishing Company, Dordrecht, 107-131, 1986.

9) Ao, T., Yoshitani, J., Takeuchi, K., Fukami, K., Mutsuura, T., Ishidaira, H., Effects of sub-basin scale on runoff simulation in distributed hydrological model: BTOPMC, Weather radar information and distributed hydrological modeling, IAHS publication no. 282, 227-233, 2003.

10) Zhang, X., Drake, N. A., Wainwright, J. and Mulligan, M., Comparison of slope estimates from low resolution DEMs: Scaling issues and a fractal method for their solution: Earth Surface Processes and Landforms, 24, 763-779, 1999.

11) Klinkenberg, B. and Goodchild, M. F., The fractal properties of topography: a comparison of methods: Earth Surface processes and Landforms, 17(3), 217-234, 1992.

(Received September 30,2003)